Influence of Powder Addition to Macrogol Ointment Japanese Pharmacopeia on the Rheological Properties

Shigeyuki ISHIKAWA* and Masao KOBAYASHI

Products Formulation Research Laboratory, Tanabe Seiyaku Co., Ltd., 16–89, Kashima 3-chome, Yodogawa-ku, Osaka 532, Japan.
Received February 26, 1990

To understand the influence of powder properties on the viscoelasticity of a powder-filled semisolid, 8 powders (zinc oxide, titanium dioxide, hydrated silicone dioxide, synthetic aluminum silicate, magnesium stearate, talc, cornstarch and glycyrrhetic acid) were added to macrogol ointment (MGO), and the viscoelasticity of the powder-filled MGO was investigated using the oscillation method at the rheological ground state and the continuous shear method at a high shear rate.

As determined by the oscillation method, storage modulus (G') and loss modulus (G'') were increased in all cases by the addition of powders, suggesting the formation of a bridge structure through the particles. Though the increasing rate of G' or G'' on the weight fraction was different from powder to powder, a good linearity was maintained between $\log G'$ or $\log G''$ and the square root of the contacting surface area ($\sqrt{S_A}$), irrespective of the powder species. A master curve between $\log G'$ or $\log G''$ and mean surface distance could be drawn. These simple relationships were more obvious than in the case of vaseline, studied previously.[1] For this difference, it was presumed that in MGO, individual powder properties such as rigidity or lubricating function were masked by the more thickly adhered layers around the particles, and these thicker layers were formed due to the high consistency of MGO.

As determined by the continuous shear method, the structures formed in MGO were susceptible to being ruptured easily. Thus, the powder properties seemed to have a stronger influence on the rheological properties at a higher shear rate than those at the rheological ground state.

Keywords macrogol ointment; powder-filled semisolid; rheology; oscillation method; continuous shear method; powder property

Rheological measurements by the oscillation method according to Onogi's theory are known to be applicable in the analysis of viscoelastic properties of many ointment bases which show nonlinear behavior.[2] In this method, storage modulus (G') or loss modulus (G'') could be obtained from the linear region of the rheograms, and these parameters are concerned with the solidity and liquidity of an ointment, respectively. The solidity and the liquidity are based on rheological concepts and are not necessarily concerned with the amount of solid or liquid materials in the vehicles. These parameters depend greatly on the nature of the structures in the vehicles formed through the interaction between particles or between particles and vehicle.

In order to understand the relationship between the structures formed in the vehicles and the rheological properties of the ointment, study using power-filled semisolids seems useful because the properties of the solid phase could be speculated by the dispersed powders. Until now, many studies have been presented on the influence of solid materials on the viscosity of ointments; however, viscoelastic evaluation under the rheological ground state should provide more detailed information about the structures. Recently, Raudebaugh and Simonelli reported such studies for powder-filled semisolids in which ZnO, starch, or colloidal sulfur was dispersed in anhydrous lanolin.[3] Their studies, while interesting and suggestive, barely mentioned the relationship between the viscoelasticity of the powder-filled semisolids and the properties of the powders used.

In the previous paper, we prepared powder-filled semisolids by adding 6 powders of various properties to vaseline. We then measured their viscoelasticity to discuss the cause of structure formation.[1] The viscoelasticity seemed to depend greatly on powder properties such as affinity to the dispersion phase, particle size, surface state, and so on.

The structure formed in a vehicle and the resulting viscoelastic properties are presumed to depend greatly on the characteristics of the ointment base. Thus, studies using other vehicles of various properties should be useful. Macrogol ointment (MGO) has different properties than vaseline. Vaseline is hydrophobic, its consistency is not as high, and it shows considerable liquid-like properties in viscoelasticity.[4] On the other hand, MGO is a representative hydrophilic ointment base, washable with water, and gives a higher consistency and smaller tan δ value than vaseline.[4] Thus, in this study, the 6 inorganic powders used in the previous study [zinc oxide (ZnO), titanium dioxide (TiO_2), hydrated silicone dioxide (Cp), synthetic aluminum silicate (SiAl), magnesium stearate (StMg), and talc], cornstarch (CNS) and glycyrrhetic acid (GA) were added to MGO and viscoelasticity was determined. Cornstarch is known to have less effect on rheological properties when it is added to lanolin.[3] Glycyrrhetic acid is made up of fine and rigid organic particles. The results using MGO are compared with those using vaseline and the difference between the two ointments is discussed considering differences of vehicle property, dispersion states, the affinities of powders to semisolid bases, and so on.

Experimental

Materials All the powders were obtained from commercial sources. ZnO, TiO_2, Cp, SiAl, StMg, and talc of the same batch to the previous paper were used.[1] In addition, cornstarch (CNS) (moisture content 12.6%, Japan Maize Product Co., Ltd.) and glycyrrhetic acid (GA) (99.1%, moisture contents 0.02%, Maruzen Pharmaceutical Co., Ltd.) were used. Densities (ρ), specific surface area evaluated by BET method (S_{BET}) and by air permeability method (S_{AP}), and particle size by Cilus method (D_{CL}) of the powders used are shown in Table I. MGO was prepared according to Japanese pharmacopeia with polyethylene glycol 400 (PEG 400) (density

TABLE I. Properties of the Powders Used in This Study

	ρ (g/cm^3)	S_{AP} (m^2/g)	S_{BET} (m^2/g)	D_{CL} (μm)
ZnO	5.74	1.57	3.33	1.1
TiO_2	3.97	2.85	8.93	0.6
StMg	1.10	1.69	4.69	15.6
Talc	2.82	1.23	2.17	12.9
Cp	2.81	10.4	145.4	13.0
SiAl	2.41	5.52	417.05	11.1
GA	1.16	3.95	11.78	5.3
CNS	1.57	0.39	0.64	13.7

1.127, Sanyo Chemical Industries, Ltd.) and polyethylene glycol 4000 (PEG 4000) (moisture contents 0.8%, Nippon Soda Co., Ltd.).

Preparation The powder-filled semisolids were prepared on a 100 g scale as follows: an equal amount of PEG 400 and PEG 4000 were weighed in a 200 ml beaker and melted at 70 °C. The melted substance was cooled to about 60 °C in 5 min under mild agitation in the Ultratarrax mixer (about 4500 rpm), then a necessary amount of powder was added. The mixture was agitated rapidly (about 8000 rpm) and was cooled gradually. At about 55 °C, where the mixture became slightly viscous, it was degassed under vacuum. Cooling was continued to room temperature under vacuum without agitation. It was difficult to assess visually whether the ointments contained bubbles or not, so the same procedure was adopted for all semisolid preparations. In order to confirm the uniform dispersion of powders, the densities of the obtained ointments were measured at several positions, the same way as the vaseline preparation. The densities were confirmed the same within the margins of experimental error, irrespective of the sampling position.

The obtained semisolids were allowed to stand at 25 °C for more than a week to attain rheological equilibrium before measurement. To establish the period required for the ointment to attain rheological equilibrium, rheological measurements of MGO containing no powders were performed for more than two weeks. The equilibrium was known to be attained within 3 d after preparation, and thereafter, rheological parameters hardly changed. Therefore, standing for more than a week at 25 °C seemed to be enough time to allow MGO-based semisolids to attain equilibrium.

Rheological Measurement Oscillation measurement was carried out at 25 °C using a Shimadzu RM-1 rheometer as described previously.[4)]

[Cone angle (ε), 7×10^{-2} rad; strain amplitude (λ), 1.75×10^{-2} rad; radius of cone-and-plate (R), 2.5 cm; torsion constant of wire (K), 6.53×10^7 dyn cm/rad; sample weight, about 3 g].

Rheological parameters G', G'', loss tangent ($\tan\delta$), and nonlinearity parameter (D_{nl}) were calculated as before by using Eqs. 1—4, respectively.

$$G'=(3Ka_1/2\pi R^3)(\varepsilon/\lambda) \quad (1)$$

$$G''=(3Kb_1/2\pi R^3)(\varepsilon/\lambda) \quad (2)$$

$$\tan\delta=G''/G' \quad (3)$$

$$D_{nl}=\left(\int_0^{2\pi}|\sigma_{obs}-\sigma_{1st}|\,d\theta\right)/\left(\int_0^{2\pi}|\sigma_{obs}|\,d\theta\right) \quad (4)$$

Continuous shear measurement was performed as reported previously using a Ferranti–Shirley viscometer.[4)]

In both methods, measurements were performed at 10 min after applying the samples to the rheometers. The rheological parameters were calculated from the first load because they usually altered with repeated application of shear.

The coefficients of variance of $\log G'$, $\log G''$, and static yield values (SYV) evaluated using MGO were 2%, 3.7% and 5%, respectively. As the rheological parameters changed greatly upon addition of the powders, these variations were small enough for the purpose of this study.

Wettability with PEG 400 Powders were packed into glass capillary tubes (diameter = 3.6 mm, length = 15 cm). The rising liquid height (h) in the tube was measured, then h^2 was plotted against time (t), and $\gamma\cos\theta$ was calculated using Eq. 5, as before.[1)]

$$h^2=(\gamma r\cos\theta)t/2\eta \quad (5)$$

where γ, r, η, and θ are surface tension, average capillary radius, viscosity of PEG 400 and contact angle, respectively.

Results and Discussion

ω Dependency of Viscoelastic Parameters Figures 1 and 2 show the dependency of G', G'', $\tan\delta$, and D_{nl} on oscillation frequency (ω) for the semisolid containing 10% of ZnO, StMg, Cp, and CNS. The former 3 were shown as representatives of powder types 1, 2, and 3 classed in the previous paper, respectively.[1)] The patterns of MGO and vaseline containing no powders were also shown for comparison in these figures.

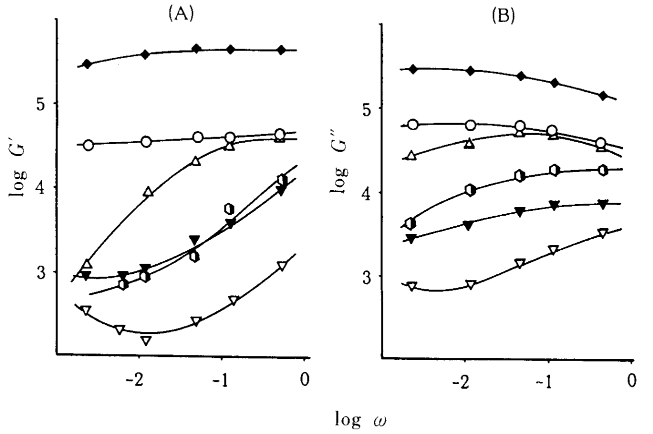

Fig. 1. ω Dependencies of Storage Modulus (G', A) and Loss Modulus (G'', B) of Powder (10%)-Filled Semisolids

Symbols: ○, ZnO; △, StMg; ◆, Cp; ◑, CNS; ▼, MGO; ▽, vaseline.

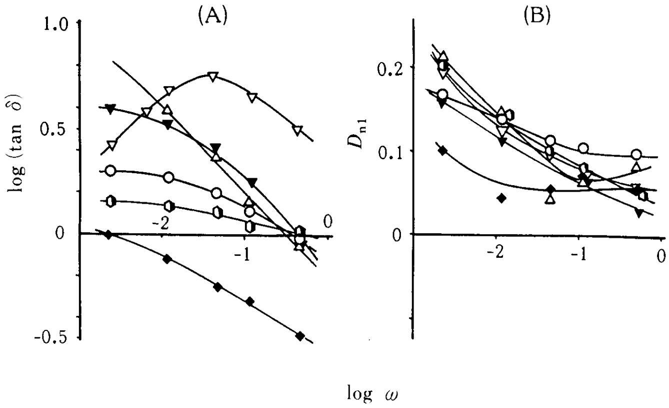

Fig. 2. ω Dependencies of Loss Tangent ($\tan\delta$, A) and Nonlinearity Parameter (D_{nl}, B) of Powder (10%)-Filled Semisolids

Symbols are same as in Fig. 1.

MGO showed higher G' and G'' values than vaseline at the whole ω range. This means MGO has higher consistency than vaseline, and this phenomenon coincides with the difference in their acceptability on skin.

The addition of Cp, ZnO, and StMg to MGO increased $\log G'$ at the whole ω range; however, CNS did not change $\log G'$ as much. The order of $\log G'$ was CP > ZnO > StMg > CNS = no additives. In vaseline, the order was Cp > ZnO > no additives > StMg.[1)] Thus, StMg behaved differently between MGO and vaseline.

The patterns of $\log G'$ of Cp and StMg on ω were similar both in vaseline[1)] and in MGO. However, in the case of ZnO, $\log G'$ scarcely increased with the increase of ω in MGO, but greatly increased in vaseline. Compared to $\log G'$s, $\log G''$s didn't change as much by changing ω in MGO.

Values of loss tangent ($\tan\delta$) were larger than 1 ($\log\tan\delta > 0$) in low ω, but they decreased with the increase of ω in all powders. This means that G'' was larger than G' and that liquidity is more dominant than solidity at low ω. The relative decrease of liquidity with an increase of ω should reflect that, if the viscoelasticity obeys the terms of the Maxwell model, dash-pot cannot react to the speed of oscillation, and consequently, the spring becomes dominant.

The patterns of $\tan\delta$ in MGO were fairly different from those in vaseline. In vaseline, $\tan\delta$ once increased and reached a maximum and then decreased as ω increased.[1] The reason for the difference in $\tan\delta$ patterns between both vehicles is not clear. However, it could be said that the patterns of $\tan\delta$ *vs.* ω of the powder-filled semisolids were similar to those of the vehicles (without any powders) on the whole.

The nonlinearity parameter (D_{nl}) showed similar patterns in both vehicles. They showed larger values up to nearly 0.2 in some cases at lower ω. This means the discrepancy from the ideal Lissajious figure was larger at small ω. As D_{nl}s were smaller than 0.1 at larger ω (when $\omega>0.1$), the following measurements were performed at 0.47 rad/s as previously.

The Influence of Powder Concentrations i) Storage Modulus and Loss Modulus The changes of elasticity and viscosity due to the addition of the various 8 powders were measured and were plotted in Fig. 3 against a weight fraction of the powders (f_p) in powder-filled semisolid using G'_R and G''_R defined in Eq. 6.

$$G'_R = G' \text{ of powder-filled semisolid}/G' \text{ of MGO}$$

$$G''_R = G'' \text{ of powder-filled semisolid}/G'' \text{ of MGO} \quad (6)$$

As shown, G'_R and G''_R increased with the addition of powders in all cases and they increased with f_p. The increasing rates at the same f_p were as follows:

$$\text{SiAl} > \text{Cp} > \text{GA} > TiO_2 = \text{ZnO} > \text{talc} > \text{StMg} > \text{CNS} \quad (G'_R)$$

$$\text{SiAl} > \text{Cp} = \text{GA} > TiO_2 = \text{ZnO} = \text{StMg} > \text{talc} > \text{CNS} \quad (G''_R)$$

In MGO, $\log G'$s were increased rapidly at low f_p and thereafter they were slowly increased by the increase of f_p (the curvatures were convex upward). Whereas in vaseline, there were regions where $\log G'$ and $\log G''$ did not change or they decreased, and thereafter they increased with the increase of f_p (the curvatures were convex downward).[1]

As shown in Fig. 3, the difference among the powders was shown more clearly in G'_R than in G''_R. Thus, the effect of the structure on the rheological properties would be reflected more clearly on G' than on G'' as discussed previously with vaseline.[1]

ii) Loss Tangent If particles are rigid enough and no special interactions occur between the MGO phase and particles, $(\tan\delta)_R$ can be written in Eq. 7 as described in the previous paper,

$$(\tan\delta)_R = 1 - \phi_p \quad (7)$$

where, $(\tan\delta)_R$ and ϕ_p mean the relative values of $\tan\delta$ of powder-filled semisolid to that of MGO and the volume fraction of powder, respectively.[3] Thus, the $\log(\tan\delta)_R$s of 8 powders were plotted against ϕ_p as determined previously (Fig. 4).

As shown, all the powders except StMg decreased $(\tan\delta)_R$, and this means that solidity increased relatively as ϕ_p increased. These patterns were greatly different from that of vaseline.[1] In vaseline, the $(\tan\delta)_R$ of powder-filled semisolid increased once, and thereafter reduced as ϕ_p increased in most cases.[1] If the point at which $(\tan\delta)_R$ begins to decrease was regarded to reflect the beginning of bridge structure formation as described in the previous paper, the decrease in $(\tan\delta)_R$ in MGO even at low ϕ_p suggested that bridge structures were formed even when the particles were few.

Besides, if the assumption set in deriving Eq. 7 were

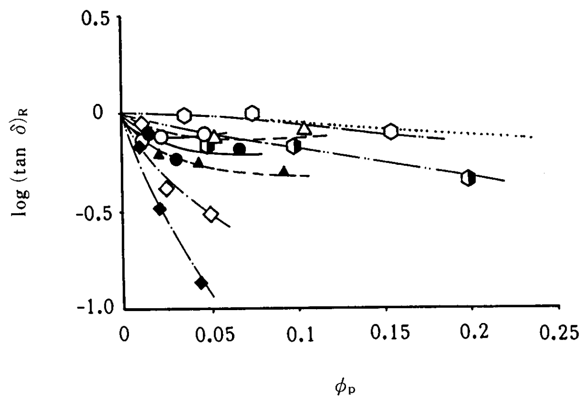

Fig. 4. Influence of the Volume Fraction of Powder for Loss Tangent
Symbols are same as in Fig. 3. ---; calculated from Eq. 7.

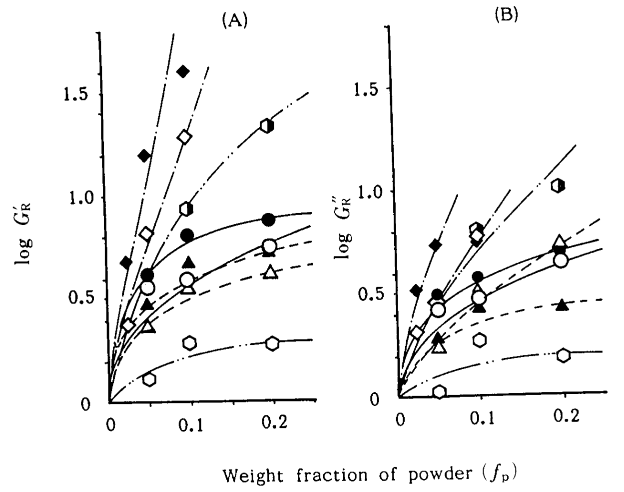

Fig. 3. Variation of G'_R (A) and G''_R (B) with Weight Fraction of Powders
Symbols: ○, ZnO; ●, TiO_2; △, StMg; ▲, talc; ◇, Cp; ◆, SiAl; ◐, G.A; ⬡, CNS.

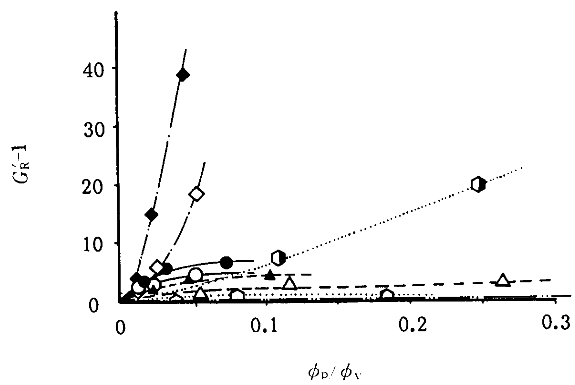

Fig. 5. Plot of G'_R According to the Kerner Equation
Symbols are same as in Fig. 3. ——--; values calculated from Eq. 8.

correct, all $(\tan\delta)_R$ values should be coincident in theoretical values (shown in Fig. 4 by dotted line). However, the $(\tan\delta)_R$s differed greatly among the powders. This also suggests that many interactions exist between the powders and the vehicles.

iii) Application of Kerner Equation According to Raudebaugh and Simonelli, the Kerner equation can be used to predict the modulus of a dispersion when particles are more rigid than the bulk phase and deformation occurs by shear.[3] It can be written as

$$G'_R - 1 = \{15(1-\mu_1)/(8-10\mu_1)\}\phi_p/\phi_v \tag{8}$$

where μ_1 and ϕ_v are Poisson's ratio of the bulk phase and the volume fraction of the bulk phase (equals $1-\phi_p$), respectively. For the dispersion of a rigid filler in a viscoelastic bulk phase that does not undergo a volume change under small strain, μ_1 is 0.5. The ϕ_p and ϕ_v values were calculated from the density of powders (ρ_p), vehicles (ρ_v), and powder-filled semisolids (ρ_{pfs}) as determined previously.[1] In Fig. 5, $G'_R - 1$ were plotted against ϕ_p/ϕ_v.

Equation 8 is based on the assumption that the particles dispersed in the bulk phase are spherical and that there is good adhesion between particles and the bulk. By comparing the observed values and the theoretical values, it was revealed that all observed values were larger than the theoretical values. This suggests that a strong interaction causing an increase of elastic structure exists between particles. The mechanism could involve a bridging whereby the parts of the molecules of macrogol interact with the surface of suspended particles and link different particles together. As the ϕ_p values increase, the probability of particle–particle contact and bridging increase, thereby providing a more structured mixture and an increase in G'.

Comparing the Kerner plotting of a powder-filled semisolid of MGO with that of vaseline, it was noticed that in vaseline, $G'_R - 1$ values agreed with the theoretical values in some powders (talc, SiAl, TiO_2) when the values of (ϕ_p/ϕ_v) were less than 0.05, and the values were less than theoretical values in StMg when ϕ_p/ϕ_v was less than 0.2.[1] However in MGO, all the powders showed higher values than the theoretical values. This suggests that bridge structures were formed more easily in MGO than in vaseline.

iv) The Influence of Interfacial Surface Area Interfacial surface area (S), which is defined as the contacting area between particles and vehicles per one gram of powder-filled semisolid, should have some effect on the viscoelasticity of a powder-filled semisolid. Thus, S was calculated using Eq. 9.

$$S = A \times f_p \tag{9}$$

where A means the specific surface area of the powders. In this study, three kinds of A were measured, that is, A_{BET}, A_{AP} and A_{CL} evaluated by the BET method, air permeability method, and Cilus measurement, respectively.

G'_R and G''_R were plotted against S calculated by all A values. As a result, the plotting of $\log G'_R$ or $\log G''_R$ against S_{AP} (calculated as $A_{AP} \times f_p$) showed a definite correlation irrespective of powder species, but plotting against S_{BET} ($= A_{BET} \times f_p$) or S_{CL} ($= A_{CL} \times f_p$) did not show an obvious relationship. Figure 6 showed the plotting of $\log G'_R$ against $\sqrt{S_{AP}}$. Fairly good linearity was shown. The line passed near the zero point.

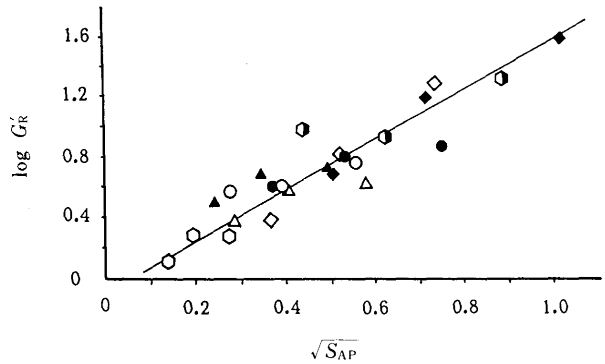

Fig. 6. The Relation between $\log G'_R$ and $\sqrt{S_{AP}}$
Symbols are same as in Fig. 3.

Table II. The Results of Least Squares Regression between $\log G'$ or $\log G''$ and $\sqrt{S}$

	$\log G'$			$\log G''$		
	$\sqrt{S_{AP}}$	$\sqrt{S_{BET}}$	$\sqrt{S_{CL}}$	$\sqrt{S_{AP}}$	$\sqrt{S_{BET}}$	$\sqrt{S_{CL}}$
a	1.515	0.135	0.413	0.918	0.055	0.643
b	−0.006	0.537	0.618	0.072	0.441	0.370
r	0.926	0.595	0.182	0.843	0.360	0.426

$\log G'$ (or $\log G''$) $= a\sqrt{S} + b$. r: correlation coefficient.

The linearity was also examined for $\sqrt{S_{BET}}$ or $\sqrt{S_{CL}}$ by the least squares method and the results were compared in Table II. $\sqrt{S_{BET}}$ or $\sqrt{S_{CL}}$ did not give a good correlation with $\log G'_R$ or $\log G''_R$.

As described in the previous paper, S_{AP} seemed to best reflect the effective surface area of powders, because S_{BET} was obtained by measuring the whole capillary tube surface, and the specific area calculated by the Cilus method (S_{CL}) might not reflect the interfacial surface area between particles and MGO because water was used as the dispersion medium and an agglomerated mass was counted as one particle.

In vaseline, the plotting of $\log G'_R$ *vs.* $\sqrt{S_{AP}}$ showed wide scattering. The linearity examined by the least squares method were as follows and the correlation coefficient (r) in vaseline was much smaller than in MGO.

$$\log G'_R = 1.52\sqrt{S_{AP}} - 0.006 \quad (r=0.93) \quad \text{in MGO}$$

$$\log G'_R = 1.41\sqrt{S_{AP}} - 0.75 \quad (r=0.66) \quad \text{in vaseline}$$

v) Influence of Mean Distance between Dispersed Particles Takano calculated the mean distance between particles (d_m) in the polyethylene gel suspension using Sharman's equation, and he examined the relationship between $\log G'$ and d_m.[5]

$$d_m = d\{(\phi_{pc}/\phi_p)^{1/3} - 1\} \tag{10}$$

where d is the volume surface diameter of the particles and ϕ_{pc} is the volume fraction of powders at the closed packing. Assuming the particles are spheres of uniform diameter, ϕ_{pc} can be regarded as 0.7405, and d is calculated from the density and S_{AP} as:

$$d = 6/(\rho \times S_{AP}) \tag{11}$$

$\log G'_R$ was plotted against d_m in Fig. 7. As shown, most points were plotted around a master curve irrespective of powder species. $\log G'_R$ increased rapidly when d_m was less than 1 μm. This means that the possibility of bridge formation is increased steeply as the distance between each particle decreases. A similar tendency was observed in $\log G''_R$.

It might be too simplified to represent the powder properties by such parameters as S_{AP} or d_m, because the circumstances around the powders were very complex. For example, the shape, the particle size distribution and the coagulation extent differ in each powder. However, the results in Figs. 6 and 7 suggested that predicting the $\log G'_R$ or $\log G''_R$ of powder-filled semisolid is in fact possible in MGO by determining such powder properties as S_{AP} or d_m.

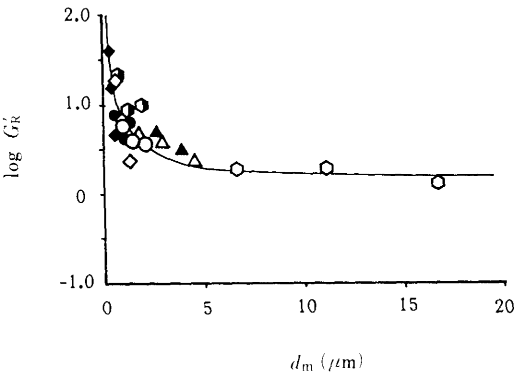

Fig. 7. Change of G'_R on the Mean Distance between Dispersed Particles in MGO

Symbols are same as in Fig. 3.

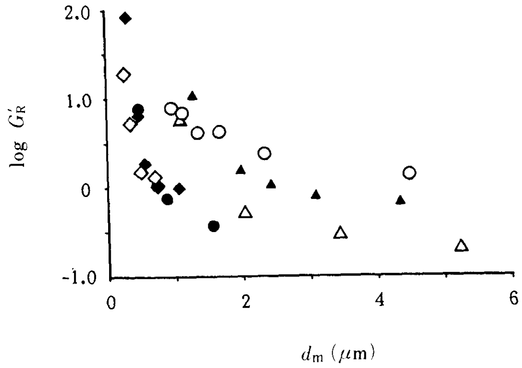

Fig. 8. Change of G'_R on the Mean Distance between Dispersed Particles in Vaseline

Symbols are same as in Fig. 3.

The influence of S_{AP} or d_m on viscoelasticity was not as simple in vaseline. In vaseline, $\log G'_R$ increased as d_m reduced, but the points were scattered more widely than in MGO (Fig. 8). It should also be noticed that all G'_Rs were larger than 1 ($\log G'_R > 0$) in MGO, whereas many of G'_R values were less than 1 ($\log G'_R < 0$) in vaseline.

vi) Affinity of Powders to MGO In the previous paper, wettability of powders to liquid paraffin was determined to explain the difference in the dispersion of powders in vaseline.[1] In this study, the affinity of powders for PEG 400 was evaluated and shown in Table III together with their affinity for liquid paraffin.

The wettability of the powders to PEG 400 was lower than to liquid paraffin, except for TiO_2. StMg especially showed low wettability for PEG 400 although it showed a high affinity for liquid paraffin. TiO_2 showed the lowest affinity to liquid paraffin and this was regarded as a cause of difference in the viscoelasticity between TiO_2 and ZnO in vaseline, although their particle sizes were nearly the same. TiO_2 coagulated in vaseline because of its poor affinity, whereas ZnO showed good dispersion.[1] In MGO, TiO_2 and ZnO showed almost the same patterns in the plotting of $\log G'_R$s against f_p (Fig. 2). The dispersions of TiO_2 and ZnO in MGO were similar, as shown in Fig. 9A and 9B, respectively.

In MGO, most of the powders dispersed well, even StMg, which showed the lowest affinity to PEG 400. Thus, wettability of powders to the vehicle seemed to have less influence in MGO than in vaseline.

The higher consistency of MGO seemed to account for the above phenomenon. Interfacial layers adhering around the particles through which the bridge structure is formed are probably thicker in MGO than in vaseline, as could be presumed from Figs. 7 and 8. In vaseline, the regression line of $\log G'_R$ against d_m crossed 0 points in most powders at less than 2 μm (Fig. 8). At this point, the effect of the powders

Table III. $r\cos\theta$ Values of Each Powder for PEG 400 and Liquid Paraffin (Liq. P)

	ZnO	TiO_2	Cp	SiAl	StMg	Talc
PEG 400[a]	5.13	0.50	0.98	3.10	0	3.35
Liq. p[a]	8.47	0.01	5.33	5.97	9.1	5.0

a) ($\times 10^4$).

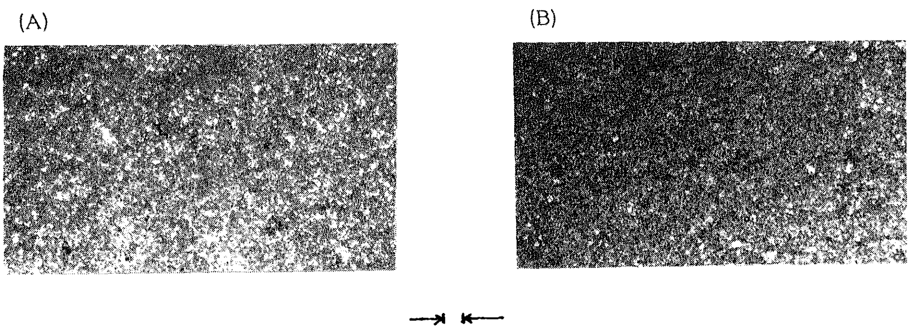

Fig. 9. Microphotographs of the Dispersion State of TiO_2 (A) and ZnO (B) in MGO

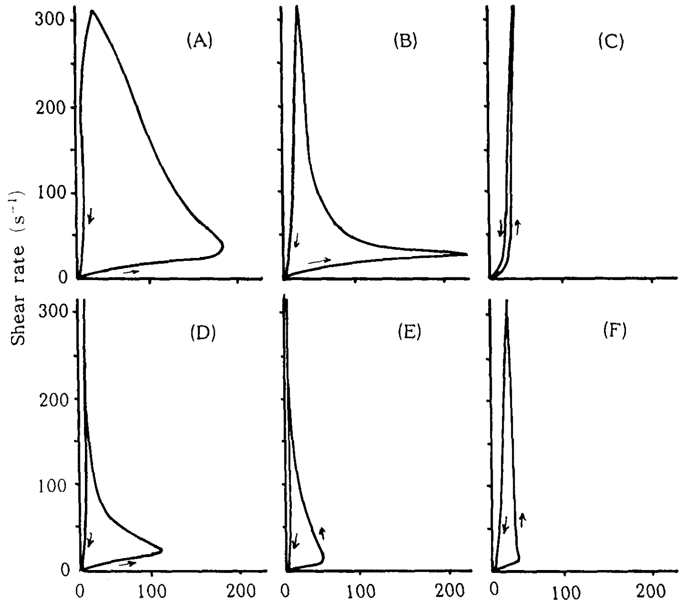

Fig. 10. Typical Flow Curves with a Ferranti–Shirley Viscometer for Powder (10%)-Filled Semisolids

(A) SiAl, (B) ZnO, (C) CNS, (D) StMg, (E) Talc, (F) MGO.

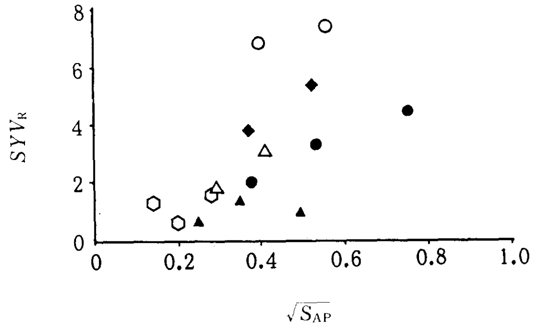

Fig. 11. Plotting of Static Yield Value Determined with a Ferranti–Shirley Viscometer *vs.* $\sqrt{S_{AP}}$

Symbols are same as in Fig. 3.

would become zero. However, in MGO $\log G'_R$ was larger than 0, even when d_m was about 17 μm, as shown in Fig. 7. If the points correspond to the maximum thickness of the interfacial layers which form bridge structures of powders, the thickness should be more than 17 μm in MGO as was supposed in Fig. 7. Thus, the properties of powders, except for surface area, were presumed to be hidden by the thick and viscous phase of the adhering layer in MGO. Consequently, there might be a fairly good correlation between $\sqrt{S_{AP}}$ and $\log G'$ (Fig. 6) or $\log G''$ (data were not shown).

The poor correlation between $\sqrt{S_{AP}}$ and $\log G'$ in vaseline might have been caused by their adhered layers. Powder properties other than surface area might also have been reflected in the viscoelasticity in vaseline.

vii) Application of Continuous Shear Method Viscoelastic measurements by the oscillation method shown in the above sections were used to evaluate at the rheological ground state. Then, the evaluation at a higher shear rate by the continuous shear method using the Ferranti–Shirley viscometer was performed for comparison. In Fig. 10, representative rheograms of powder-filled MGO were shown.

MGO and most of its powder-filled semisolids showed a marked difference between the rising curves and the falling curves. This means that they have many thixotropic properties, and the structures formed in the vehicles were easily ruptured by the addition of high shear.

As rheological parameters, the static yield value (SYV), which was determined at the spur point, and the viscosity at a shear rate of 319 s^{-1} (η_{319}) were estimated, and the correlation between relative SYV values (SYV_Rs) or η_{319} *vs.* $\sqrt{S_{AP}}$ were investigated. In the results, an obvious relationship was not observed in the latter case, but in the former case it was observed that as a general tendency, the SYV_R increased with an increase of $\sqrt{S_{AP}}$ (Fig. 11), though the linearity was not as good as in the case of $\log G'_R$ (Fig. 6) or $\log G''_R$ (data were not shown). As shown in Fig. 11, ZnO produced the highest SYVs among powders. However, the shear stress (σ) decreased very rapidly with an increase of shear rate after the spur point (Fig. 10). Static yield values indicate the stress necessary to break the structures existing at the static state. The largest SYV_R of ZnO reflects that the structures formed by ZnO are very rigid. Many factors could explain this rigid structure, such as the dispersion state of particles, the numbers of contacting points between particles, and so on. In addition, the rigid property of a ZnO particle, which is presumable according to its high density (Table II), is significant. It is not unreasonable to assume that powder properties are translated more of less to that of whole powder-filled semisolid through the powder contacting point. However, if the structure is once destroyed by the shear (γ), reconstruction of the structure seems difficult in a shear-imposed state. The powder properties of ZnO, such as surface smoothness or weak powder–powder entanglement ability, are presumed to have an effect on this phenomenon in addition to surface area.

SiAl produced slightly lower SYVs than ZnO, but the decrease of σ with the increase of γ after the spur point was slow compared with that of ZnO. Therefore, the structure of SiAl was not so stiff, but it was not so fragile as that of ZnO at higher shear either. Because of this phenomenon, the powder properties of SiAl should be discussed. The particles of SiAl are not as rigid as those of ZnO, as presumed from the density, but its surface is probably very rough, as presumed from the large specific surface area by the BET method. It is presumed that the bridging structures are formed through the entanglement of protuberances in the shear-imposed state and this would explain why SiAl is less fragile than ZnO at higher shear.[4)]

In the case of CNS, the difference between the rising and falling curves was reduced, compared to the case of MGO itself. For this interesting phenomenon, the smoothness in surface and fairly larger particle size of CNS might be the cause. In addition, CNS may change its shape to correspond with additions since the particles of CNS are soft.

In the case of StMg and talc, the SYVs were moderately high. This probably reflects the moderately high rigidity of the structure constructed at the static state. However, once these structures are destroyed by adding γ, the σs are rapidly decreased to be smaller than that of MGO itself. This phenomenon might be accounted for by the fact that both of them have great lubricating capabilities. Slippages between the particles or between particle and vehicle might occur.

From the above results, the properties inherent to the respective powders seemed to be exposed to some extent by the continuous shear method, especially at a higher shear rate. By the oscillation method, G' and G'' were related with such common physical properties as S_{AP}, but the special powder properties such as lubricating function, roughness or softness were not reflected on G' and G''. For this reason, it was presumed that the thick adhered layers of MGO around particles existing at the rheological ground state were reduced by adding a high shear and thus the powder properties of each additive could be more clearly observed. Therefore, the determination of rheological properties in combination with the oscillation method and the continuous shear method offered useful and interesting information about the structure of the powder-filled semisolids.

References

1) S. Ishikawa, M. Kobayashi and M. Samejima, *Chem. Pharm. Bull.*, **37**, 1355 (1989).
2) S. Onogi, T. Masuda and M. Matsumoto, *Trans. Soc. Rheol.*, **14**, 275 (1970).
3) G. W. Raudebaugh and A. P. Simonelli, *J. Pharm. Sci.*, **73**, 590 (1984); *idem*, *ibid.*, **74**, 3 (1985).
4) M. Kobayashi, S. Ishikawa and M. Samejima, *Chem. Pharm. Bull.*, **30**, 4468 (1982).
5) M. Takano and H. Kambe, *Bull. Chem. Soc. Jpn.*, **37**, 89 (1964).